



**HAL**  
open science

## A New Bio-Inspired Hybrid Cable-Driven Robot (HCDR) to Design More Realistic Snakebots

E. Gautreau, J. Sandoval, X. Bonnet, M. Arsicault, S. Zegloul, M.A. Laribi

► **To cite this version:**

E. Gautreau, J. Sandoval, X. Bonnet, M. Arsicault, S. Zegloul, et al.. A New Bio-Inspired Hybrid Cable-Driven Robot (HCDR) to Design More Realistic Snakebots. 2022 IEEE International Conference on Robotics and Automation (ICRA 2022), May 2022, Philadelphie, PA, United States. pp.2134-2140, 10.1109/ICRA46639.2022.9811550 . hal-04016712

**HAL Id: hal-04016712**

**<https://hal.science/hal-04016712v1>**

Submitted on 12 Apr 2023

**HAL** is a multi-disciplinary open access archive for the deposit and dissemination of scientific research documents, whether they are published or not. The documents may come from teaching and research institutions in France or abroad, or from public or private research centers.

L'archive ouverte pluridisciplinaire **HAL**, est destinée au dépôt et à la diffusion de documents scientifiques de niveau recherche, publiés ou non, émanant des établissements d'enseignement et de recherche français ou étrangers, des laboratoires publics ou privés.

# A new bio-inspired Hybrid Cable-Driven Robot (HCDR) to design more realistic snakebots

E. Gautreau, J. Sandoval, X. Bonnet, M. Arsicault, S. Zeghloul, M.A. Laribi

**Abstract** - Bioinspired robots are useful tools to study complex biomechanical processes of animal locomotion. Key movements and main kinematic parameters are under the control of experimenters, which is impossible to perform when experimenting with living animals. The primary challenge to test biological hypotheses is to design realistic robots. Many snake species are proficient swimmers; they inspired the building of aquatic snakebots. Yet, underlying biomechanics of undulatory swimming which involves the whole body, i.e., anguilliform swimming, remains poorly understood. Most of the underwater snakebots designed so far are made of rigid segments articulated with joints that form a broken-line system, while the skeleto-muscular systems of living snakes include more than 200 overlapping vertebral-musculotendinous units, conferring an extreme flexibility and fluidity. This paper introduces a novel design based on flexible hybrid continuum cable driven robot (HCDR) developed through tight interactions between biologists and roboticists. This Biology-Push bio-inspired design significantly increases the fluidity and freedom of movements of the robot. Improved mimic natural snake's locomotion is therefore given using cable-driven transmissions to represent linkages between muscles, tendons, and vertebrae providing good fluidity, unlike common swimming snake-like robots made of rigid links. In addition, the association of rigid and flexible parts allows a more homogeneous distribution of actuators and masses needed to design autonomous swimming snake robot. Combining literature data and original analyses of the kinematic of swimming snakes, we inferred and implemented a kinematic model in the prototype to control movements in a plane and in a volume. Finally, we compared the resulting swimming kinematic of the device with actual snake's movements.

**Index Terms**— Biomimetics, compliant joint, snake-like robot, continuum robot, redundant robot

## I. INTRODUCTION

**B** IOMIMETICS, refers to novel technologies inspired from the study of specific adaptations of living organisms facing various challenges [1]. This scientific field rapidly developed during the past decades, for instance ISO standard 18458:2015 now provides a conceptual framework of biomimetics [2]. Many drones or technical improvements have been bioinspired from animal locomotion [3]. For example, development of underwater bio-inspired robots, called Autonomous Underwater Vehicles (AUVs), is expending rapidly over the past years [4].

Bioinspired robotic models are based on biological models, at least partly. Reciprocally, robotics offers powerful tools to address biological hypotheses [5]. However, interactions between biologists and roboticists remain often limited while the complementarity of biological and robotic disciplines is promising [5]. Such interactions were important in this paper. The current study begins with the analysis of several anatomical traits and of swimming characteristics of living snakes [6] [7] as available information on swimming kinematic is limited. Thus, we used video processing to extract qualitative and quantitative kinematic data of swimming snakes. Other methods offer means to further assess snake's aquatic locomotion; for example motion capture (MoCap), accelerometer fitting [8], X-Ray analysis [9], PIV (Particles Image Velocimetry) [10], electromyography [11] or Scanning Electron Microscopy (SEM) [12].

Pioneer studies of Shiego Hirose influenced the development of snake-like robots [4]. Currently, the design of underwater snake-like robots is mainly achieved through an assembly of identical modules linked with spherical or universal active rigid joints [13] or passive twist joints for ACM-R5 [4]. While this design provides satisfactory swimming autonomy and a homogeneous distribution of actuators along the snakebot, it lacks fluidity and thus shows limited biomimicry characteristics. Each module embeds at least one gear actuator, the snakebot can swim in a plane (Amphibot II) [14] or in a volume (Mamba robot) [15]. Eel-like robot [13] is made of three actuators for pitch, yaw and active twist to increase fluidity. The design of such robot tends to include soft electric actuators (SEA) [16] or artificial muscles [17] to obtain compliant and fluid motion. Contrary to rigid links, soft robotics emerge with the design of soft cable-driven continuum manipulators [18]. This design allows curvatures of the body and fluid motions using a series of compliant joints [19]. However, the actuators of each section are deported out of the robot base and are not homogeneously distributed, entailing a lack of autonomy for snake AUVs. Moreover, the use of flexible materials

E. Gautreau, M.A. Laribi, J. Sandoval, M. Arsicault and S. Zeghloul are with the Department GMSC of the Pprime Institute, CNRS - University of Poitiers - ENSMA, Poitiers, PC: 86000, France (e-mail: elie.gautreau@etu.univ-poitiers.fr; med.amine.laribi@univ-poitiers.fr; juan.sandoval@univ-poitiers.fr; marc.arsicault@univ-poitiers.fr; said.zeghloul@univ-poitiers.fr).

X. Bonnet is with the team ECOPHY of the Center for Biological Studies of Chizé, UMR 7372 CNRS – University of La Rochelle – PC: 79090, France (email: bonnet@cebc.cnrs.fr)

combined with a rigid skeleton [3] is recommended to be comparable to biological systems. Thus, to attain high level of biomimicry, artificial locomotor systems should involve soft materials or linkage, in association with muscle-like actuators to reproduce natural motion fluidity.

Currently, most snake-like robots are made of a series of identical rigid modules [15] [16] [13]. A module is a section of the snake robot that can be added or removed from the robot's body. An independent joint is used to reproduce the number of degrees of freedom identified on a biological snake (usually between 1 and 2 Degrees of freedom). A module contains a joint and one or more drives. Empirical and experimental studies of snake's morphology and locomotion are essential to design realistic module. Then, collaboration with biologists becomes essential to design realistic underwater snakebots and assess the consequences of design choice. Motion control of cable-driven module (the elementary part of a whole swimming snake-like robot) can be achieved throughout the kinematic model [20]. Literature suggests that three main locomotion strategies are used to control whole underwater snake robot motion [21]. 1) The use of kinematic model allows each module to be controlled independently. 2) The propagation of sinusoid waves creates undulatory motion which is a straightforward mathematical equation applied to each module with a delay induced between each of them. 3) The motions inspired from biologic neural networks like Central Pattern Generator (CPG) [14] reproduces cyclic motion.

The main contributions of this paper were to develop a new bio-inspired snake-like robot, designed in close collaboration with biologists, and to combine the advantage of the association of a flexible joint to a rigid part. The cable-driven module design is inspired from the natural linkage between muscles, tendons, and vertebrae. The HCDR module offers modularity, fluidity and enables homogeneous distribution of actuators (mass distribution) in the perspective of autonomous swimming. We used Rigid Body Replacement method [22] to design bio-inspired flexible module (BFM) made of complex compliant joints, notably to reproduce changing curvatures of the body of moving snakes. A biomimicry approach with video processing algorithm was developed to extract body's curvature of swimming snakes, and then to design the HCDR module. To our knowledge, developing a method to mimic snake's skeleton curvature (that determines snake's body curvature) during swimming based on measurements collected on real swimming snakes (hence deeply linking biology to robotics) was not previously undertaken.

This paper is organized as follows. Snake analysis section II deals with the assessment of snake anatomy and snake swimming. In section III, the module design of a snake-like robot is introduced, notably to describe BFM sizing with theoretical, numerical, and experimental coupling. Besides, the robot kinematic models are presented. In section IV, experimental results on the module's movements are compared with those obtained with snakes. Finally, Section V and VI propose future work and conclusions respectively.

## II. SNAKE ANALYSIS

Here, biomimicry involves two main criteria: the study of the snake's anatomy and the study of swimming snake's locomotion. We extracted relevant data (velocity, angles amplitude, radius amplitude) to design the robot and establish mechanical equivalency between moving snakes and robotics.

### A. Snake anatomy

On average, a snake is composed of 100 to 300 vertebrae according to species and sex. Figure 1 shows how vertebrae are articulated with hemispherical parts (centrum) and pairs of zygapophyses (facets of vertebrae that articulate with corresponding facets of adjacent vertebrae). Vertebrae are inter-connected with complex assemblage of ligaments and cartilages (not shown). This allows flexion-extension, lateral bending, and a small torsion amplitude. It is therefore possible to consider this link as a ball joint (3 DoF of rotations). Note that a small compression of the spine, that reduces spine flexibility, adds an extra degree of freedom [23]. In fact, it can be considered as a sliding joint. Nevertheless, compression motion is a very complex kinematic and is not the most relevant movement for the undulatory locomotion of snakes. Therefore, this link will not be considered for the design of the robot. Instead, we focus on the ball joint from centrum.

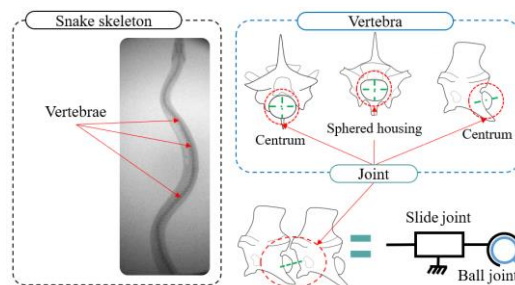


Fig. 1. Snake vertebrae articulation equivalence with mechanical joints. Here, a slide joint plus a ball joint is the equivalence of a snake intervertebral joint.

Also, snakes can actively modify their body shape by compressing laterally the posterior half of their body during swimming, [24]. Such dynamic process along with the diversity of snake's body shape likely substantially contribute to snakes swimming efficiency (e.g. optimizing thrust propulsive versus resistive drag). Yet, their possible influence on swimming kinematics is not known. Therefore, in this study that focuses on kinematic, they were discarded. Thus, only ball joints and body curvature of snakes will be considered in this study.

## B. Snakes swimming kinematics

Swimming styles of many animals are classified into three main categories: propulsion with Body Caudal Fin (BCF) oscillation, propulsion with body undulation, and propulsion by water jet/expulsion [3]. Snakes adopt an oscillating mode of propulsion that involves the whole body, or anguilliform swimming [25].

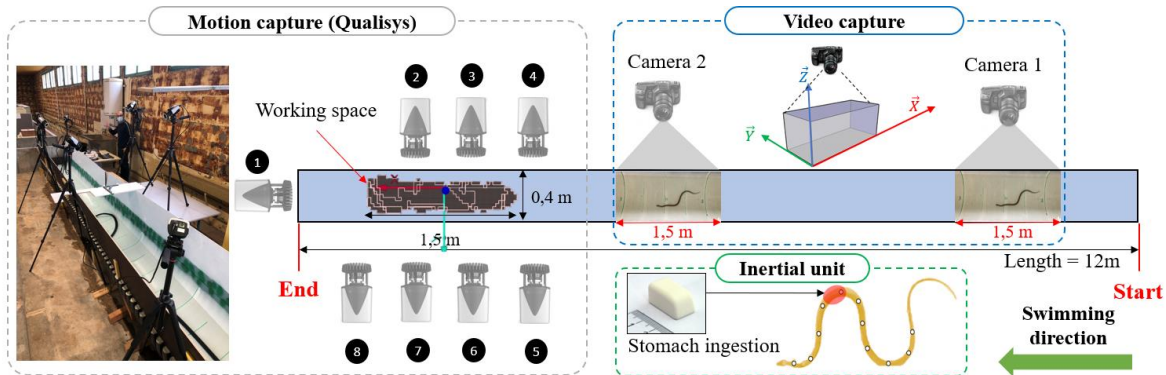


Fig. 2. Swimming bench composed of motion capture, video capture and inertial unit

Video footage, MoCap and accelerometers were used to record swimming characteristics of snakes tested in a 12 meters swimming pool (Fig. 2). MoCap was performed with a Qualisys setup system. Eight infrared cameras covered a working space of  $1.5 \times 0.4$  m. Two Gopro Hero 9 cameras ( $1980 \times 960$  pix, 240 fps) were placed in the first half of the pool to record swimming snakes from above (1.5m). One grass snake (*Natrix helvetica*) and two whip snakes (*Hierophis viridiflavus*), were captured in the Chizé forest. They were kept in captivity for a period of 2 to 3 days during trials. The grass snake is a terrestrial species that exhibits aquatic habits; the whip snake is terrestrial. Each snake swam 7 to 10 times (70 to 100 m in total). We used only sequences during which the snakes swam regularly (e.g., no stop).

A video processing algorithm was developed to analyze video footage using OpenCV library. First, a video footage is sliced into an image sequence. Each frame is binarized to extract snake shape and skeletonize the shape. The skeleton is a set of points passing through the center of the snake along its length (i.e., a mid-body line represents the spine). A polynomial interpolation of degree 9 is applied to the skeleton. The obtained line virtually represents the skeleton of the animal. A sequence of interpolated curves represents the movement of the snake. Second, snake's body oscillating frequency ( $f$ ) computed from the head point for multiple periods, head amplitude ( $A_{moy}$ ), and transversal ( $V_{t,moy}$ ), longitudinal ( $V_{l,moy}$ ), and resulting ( $V_{r,moy}$ ) head velocity of swimming snake are extracted (as shown in Table 1). Velocities are calculated by numerical derivatives for each point of the skeleton from frame  $n-1$  to frame  $n+1$ . Longitudinal velocity is the velocity calculated in the swimming direction (along X-axis) while transversal velocity is the velocity perpendicular to swimming direction (along Y-axis) (Fig. 2). Finally, video analyses give access to the whole snake movements (Fig. 3).

Table. 1. Extracted data from video capture on *Hierophis viridiflavus* (3).

$f$ (Hz)	$A_{moy}$ (m)	$V_{t,moy}$ (m/s)	$V_{l,moy}$ (m/s)	$V_{r,moy}$ (m/s)
0.89	0.05	0.16	0.45	0.48

A snake-like robot is made of multiple modules, as depicted in the segmentation of snake skeleton (Fig. 3). This representation of each module allows extracting angles during snake locomotion (Table 2). However, a straight segmentation does not fully mimic the fluidity of snake movement. To cope with this issue, an arc interpolation of each segment was performed (Fig. 4). The arcs approximate the curvature adopted by snake's body during swimming. Some arcs centers are not displayed because radius would be out of plot range in fig. 4. Radius's values were calculated for different swimming sequences (Table 2).

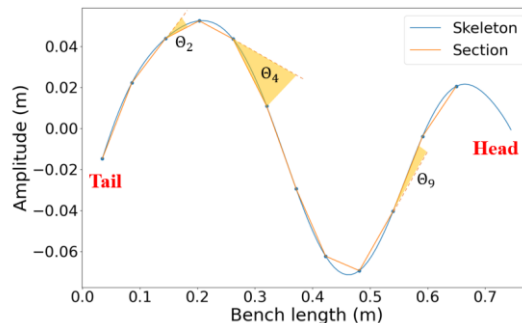


Fig. 3. Snake segmentation with straight sections and relative angles between each section.

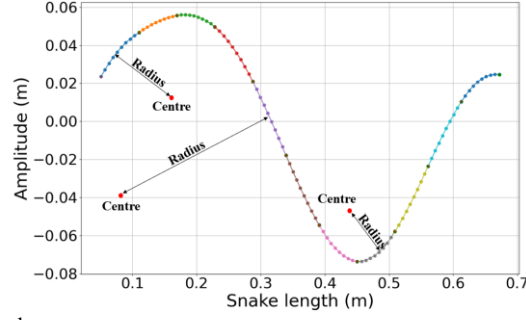


Fig. 4. Arc interpolation of each section for one snake.

Table. 2. Angles and radius from segmented snake analysis for a given velocity. (1) *Natrix helvetica*, (2) and (3) *Hierophis viridiflavus*. (1) swam 10 times (100 meters) and 1 video analyzed: third swim. (2) swam 10 times (100 meters) and 1 video analyzed: second swim. (3) swam 7 times (70 meters) and 1 video analyzed: fourth swim. Extracted values are computed with snake segmentation of 11 sections.

Snake	$V_{r_{moy}}$ (m/s)	Max angle (deg)	Min angle (deg)	Max radius (m)	Min radius (m)
(1)	0.56	41.44	0.01	36.27	0.07
(2)	1.19	47.71	0.01	582.3	0.11
(3)	0.48	33.73	0.02	249.13	0.14

The preliminary results obtained can be used in robotics. The movements of the snake are mimicked through each section interpolated by an arc. Thus, each section corresponds to a bio-inspired module moving in a plane or in a volume. A snake robot is the result of the assembly of several HCDR modules. In the following sections, the obtained measurements on swimming snakes (Fig. 2) will be compared with those obtained with the bio-inspired module put in motion.

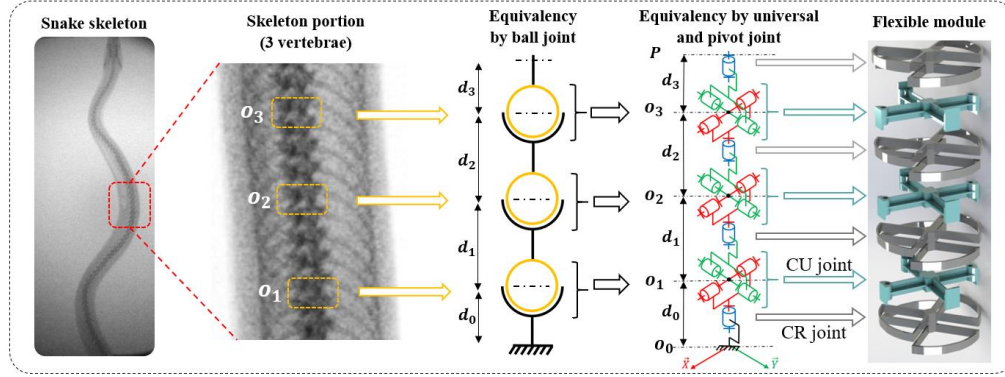


Fig. 5. Description of RBR (Rigid Body Replacement) method from snake skeleton to flexible module composed of compliant revolute joints (CR joints) and compliant universal joints (CU joints).

### III. BIO-INSPIRED MODULE DESIGN

The design of the bio-inspired HCDR module must precisely reproduce snakes' swimming locomotion and snakes' skeleton curvature. Figure 6 shows the HCDR module design (Fig. 6 – b) combining one 3D printed Bio-inspired Flexible Module (BFM) (Fig. 6 – c) composed of compliant vertebrae and two rigid modules (Fig. 6 – a) composed of two servomotors (Dynamixel 2XL-430-W250-T). Servomotors are mounted in opposition and placed perpendicularly from each other to control module's bending in each plan through pulley angles acting on cables length. The Dynamixel servomotor (Fig. 6 – a) is a universal joint composed of two DoF (2 servomotors). Each servomotor is linked with the flexible module by a 3D printed mounting (Fig. 6 – a). Each of the two motors of one servomotor drives two antagonistic braided Nylon cables wound in opposite directions on a single pulley. In fact, the module bending on a plane is achieved through the rotation of a pulley. The latter drives the winding of a cable and the release of the antagonist cable. Cables are passing through the beams of the flexible vertebrae (Fig. 6 – c). A tensioning system allows the length and tension of the cables to be adjusted.

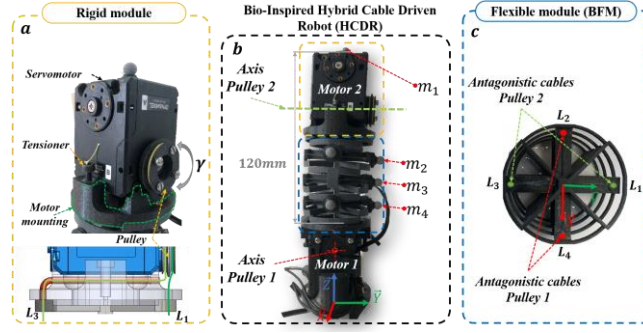


Fig. 6. Bio-inspired Hybrid Cable Driven Robot (b) composed of two rigid modules (a) and a flexible module (BFM) (c). “m” stands for marker.

### A. Bio-inspired Flexible Module (BFM) sizing

Biomimicry is applied using Rigid Body Replacement (RBR) method [22] to design BFM. This schematic method allows replacing rigid mechanical joint by complex compliant joint. Here, we arbitrary used three vertebrae. Figure 5 shows the application of RBR method to design an equivalent flexible module composed of compliant revolute (CR) joints and compliant universal (CU) joints.

BFM mainly works in flexion-extension and lateral bending. Thus, CU joints which are the most used joints are well suited to the targeted movements. The coupling of a theoretical, numerical, and experimental study enables sizing one CU joint and the module in terms of bending angles and curvature. Each CU joints is made of two orthogonal beams each working in torsion as shown in Fig. 7. Beam shape was inspired from [26]. PA11 Selected flexible material sustains large magnitude compliant flexible motion and resists cyclic bending.

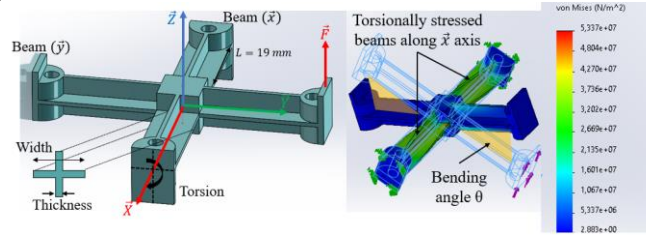


Fig. 7. General shape of CU joint.  $\vec{F} = 7.5N$  is applied to the beam.

Maximum bending angle  $\theta_{max}$  is determined, using Eq. (1-2), according to the maximum torque  $\tau_{max}$  applied on the beam through a force  $\vec{F}$ , the torsional stiffness  $K_\theta$ , and the beam parameters:  $w$  the width and  $t$  the thickness.

$$\theta_{max} = \frac{\tau_{max} Q}{2K_\theta} \quad (1)$$

$$K_\theta = \left( \frac{w}{t} - 0.373 \right) \frac{4Gt^4}{3L} \quad (2)$$

Where  $Q = \frac{w^2 t^2}{3w + 1.8t}$  and  $G$  is the Coulomb's modulus. Absolute angle of the BFM is considered as the sum of angles from each beam as follow  $\Theta = 3\theta$ .

The second part of the coupling is a finite element design on both, beam ( $t=0.7mm$ ,  $w=7mm$ ,  $L=19mm$ ) and BFM. Different loads are applied on one beam (Fig. 7) to reach Tensile Strength:  $54 Mpa$  of Nylon PA11. This limit is used to determine the maximum load applied to a beam (7.5N) in order to adapt the tension applied by the servomotor. Finite element analysis is performed under SolidWorks to study the total deformation of the BFM under different loads. The force  $\vec{F}$  applied on the module corresponds to that of the cable pulling the module as shown in Fig. 8. The relative bending angles between CU joints are not constant. Absolute angles ( $\Theta$ ) are measured using SolidWorks and compared (Fig. 10).

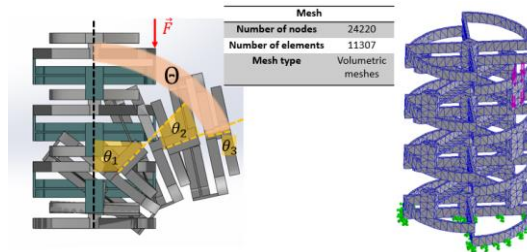


Fig. 8. BFM deformation ( $\vec{F}=3N$ ).

We experimentally compared the behavior of two BFM's manufactured models that were 3D printed in one-piece of Nylon PA11 using the dimensions obtained from the analytical and finite element studies. The first module was printed using Selective Laser Sintering (SLS) manufacturing process. A second module was printed using Multi jet Fusion (MJF) process. Figure 9 shows the test bench procedure where different loads from 20 to 200 grams were applied on the flexible module. The loading tests gave access to the relative angles ( $\theta$ ) and absolute angles ( $\Theta$ ) of each 3D printed module (Fig.10). The angles were calculated by tracking 4 markers  $m_i$  (Fig. 6) fixed on each torsional beam using the Qualisys MoCap system (Fig. 9).

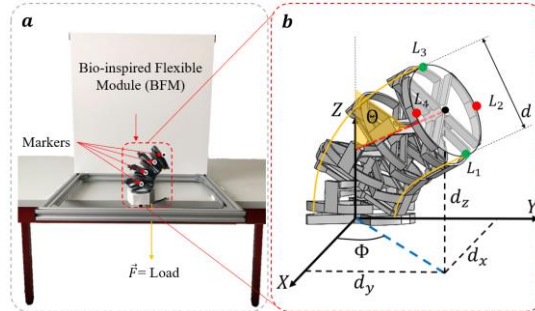


Fig. 9. (a) Absolute angle measured on a 3d printed MJF Bio-inspired Flexible Module (BFM) using MoCap system according to different loads ( $\vec{F}$ ). 4 markers are placed along HCDR Module (underwater snake robot section) to compute relative and absolute angles. (b) Space correlation representation between actuators space and workspace.

Figure 10 shows absolute angles according to load obtained by theoretical, numerical, and experimental approaches. Results obtained with 3D printed MJF module were closer to the theoretical and numerical outcomes compared to those obtained with SLS module. Indeed, the post-treatment (bead blasting) after printing erodes the surfaces of the SLS module and reduces the thickness of the module walls contrary to the MJF module which remained intact. Erosion increases the flexibility of the SLS module, hence the offset observed in Fig. 10 for a load of 0.2N.

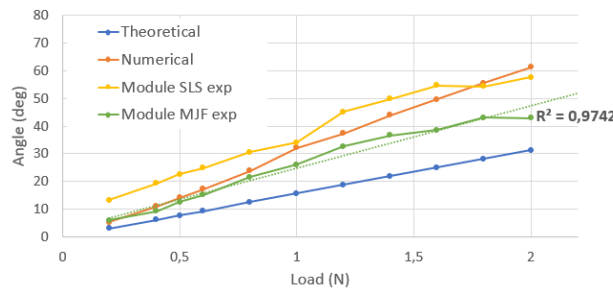


Fig. 10. Comparison of absolute angles according to load.

Outcomes from experimental suggest a linear deformation (correlation coefficients close to 1), similar to the theoretical results. While relative angles were not completely identical, BFM MJF module adopt the form of an arc (Fig. 11) whose radius and center vary with the load. Constant curvature response is necessary to apply Inverse Kinematic Model. Figure 11 shows the radius range calculated using markers crossing through arcs on MJF module. The curvature of the module reproduces all curvature of arc-interpolated sections measured on the snake skeleton during swimming (Fig. 4 and Table 2). Minimum radius of the BFM module was 50 mm while minimum radius of snakes was 70 mm. Maximum radius corresponds to the module in vertical direction.

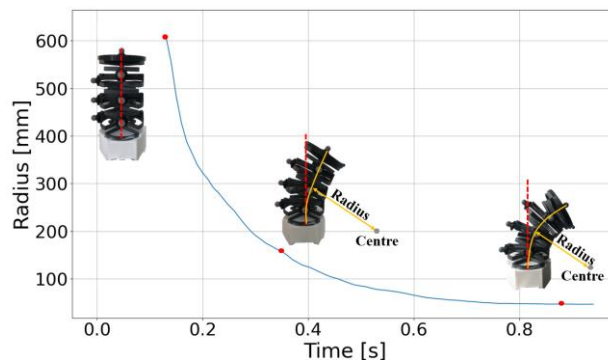


Fig. 11. Radius according to time Radius come from marker fitting by arc. Module is actuated through the cable from initial state to maximum curvature.

## B. Robot kinematic models

The motion of the hybrid module via simple or complex trajectory generation involves kinematic models. In this section, we present the mathematical models [20] adapted to the HCDR module. It consists of linking the length of the cables ( $L_1, L_2, L_3, L_4$ ) to the Cartesian position ( $x, y, z$ ) of the extremity of the effector  $p$  (Fig. 12). Cable locations are shown in Fig. 6.

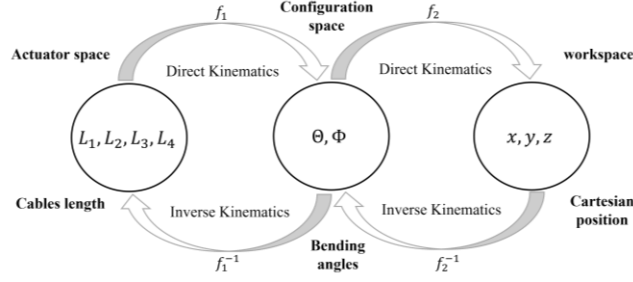


Fig. 12. Kinematic mapping of the different spaces

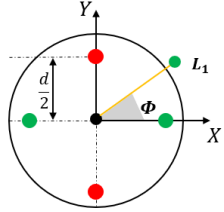
Direct kinematic model (DKM) links actuator space (cables lengths) with configuration space (bending angles) and working space (Cartesian positions). Figure 9 shows space correlation by linking cable lengths to angles. The following equations can be deduced for the direct kinematics:

$$\begin{cases} \Phi = \text{atan}\left(\frac{L_2 - L_4}{L_1 - L_3}\right) \\ \theta = N \cdot \theta = 2N \cdot \text{asin}\left(\frac{\sqrt{(L_1 - L_3)^2 + (L_2 - L_4)^2}}{2N \cdot d}\right) \end{cases} \quad (3)$$

$$\begin{cases} x = \cos \Phi \left[ \sin\left(\frac{\theta}{2}\right) d_1 + \sin\left(\frac{3\theta}{2}\right) d_2 + \sin\left(\frac{5\theta}{2}\right) d_3 \right] \\ y = \sin \Phi \left[ \sin\left(\frac{\theta}{2}\right) d_1 + \sin\left(\frac{3\theta}{2}\right) d_2 + \sin\left(\frac{5\theta}{2}\right) d_3 \right] \\ z = d_0 + \cos\left(\frac{\theta}{2}\right) d_1 + \cos\left(\frac{3\theta}{2}\right) d_2 + \cos\left(\frac{5\theta}{2}\right) d_3 \end{cases} \quad (4)$$

Here,  $N$  is the number of cables,  $d$  is the cable distance between antagonistic cables and  $d_0, d_1, d_2, d_3$  are the distances between flexible vertebrates (Fig. 5).

Inverse Kinematic Model (IKM) is applied to link cartesian positions of the end effector as input with servomotors pulley angles as output. Cartesian positions, representing a given trajectory, are defined as inputs to calculate the bending angles, cables lengths and thus the rotation angles of the pulleys (output). The following equations can be defined as:

$$\begin{cases} \theta = \frac{1}{N} \cdot \text{atan}\left(\frac{\sqrt{x^2 + y^2}}{z}\right) \\ \Phi = \text{atan}\left(\frac{y}{x}\right) \end{cases} \quad (5)$$


$$\begin{cases} L_1 = L_0 + 2N \left(\frac{d}{2} \cos \Phi \sin\left(\frac{\theta}{2}\right)\right) \\ L_2 = L_0 + 2N \left(\frac{d}{2} \sin \Phi \sin\left(\frac{\theta}{2}\right)\right) \\ L_3 = L_0 - 2N \left(\frac{d}{2} \cos \Phi \sin\left(\frac{\theta}{2}\right)\right) \\ L_4 = L_0 - 2N \left(\frac{d}{2} \sin \Phi \sin\left(\frac{\theta}{2}\right)\right) \end{cases} \quad (6)$$

Fig. 13. Robots bending in an arbitrary direction [20].

Here,  $L_0$  is the initial length of the cables.  $P_i, i \in \{1,2,3,4\}$  represent the waypoints where the cables pass through the flexible module. Cables used are Dyneema® SK71 braided lines with a diameter of 0.21mm. We consider an infinite stiffness because of its high resistance. The length of the cable  $i$  is linked with the rotation angle of the pulley  $\gamma_i$  (Fig. 6) as follow:

$$\gamma_i = -L_0 + \frac{L_i}{r} \quad (9)$$

With  $i \in [1,2,3,4]$  cables and  $r$  the pulley radius.

## IV. EXPERIMENTATIONS

In this section, the robot kinematics models are used to generate two trajectories in order to assess the module abilities in reproducing motions measured on snakes. Trajectories are defined to evaluate: (1) how well the module mimics snake section angles and anguilliform planar motion measured in living snakes. (2) To what extent the module movements in the longitudinal



and transversal planes reproduce the three-dimension motion of a swimming snake. MATLAB is used to drive the servomotors.

### A. Experimental trajectories

The first implemented trajectory was a circular planar arc ( $\mathbf{X}, \mathbf{Z}$ ) (Fig. 9), obtained by activating one servomotor and with a maximal inclination of HCDR module (absolute angle  $\Theta$ ) of  $60^\circ$ . Angles  $\gamma_2$  and  $\gamma_4$  of the pulley, acting on cable lengths  $L_2$  and  $L_4$  respectively, were actuated by the servomotor 1 (Fig. 6). Cables  $L_1$  and  $L_3$  are antagonistic and wound to the same pulley and angles  $\gamma_1$  and  $\gamma_3$  of the pulley are actuated by servomotor 2. These angles are null as the pulley is fixed to perform the planar motion. Figure 14 shows the relationship between the absolute angle  $\Theta$ , measured between the marker  $m_1$  and the vertical axis ( $Z$ ) and the resulting configuration of the bio-inspired flexible module's curvatures. Four positions, (1), (2), (3) and (4) were selected to illustrate this relationship.

Servomotor 1 is active and bends the BF module. The upper servomotor is passive and brings a payload to support the end effector. Figure 15 shows that the theoretical and experimental trajectories are continuous and that they overlap. Measured absolute angles shows the module capacity to move across a wide range of angles. The HCDR is able to cover the angle range ( $33.73^\circ$ ) extracted in swimming *Hierophis viridiflavus* up to  $35^\circ$ , as reported in Fig. 14. The HCDR presents a high capability to mimic other snakes, notably (1) and (2), through a simple customization.

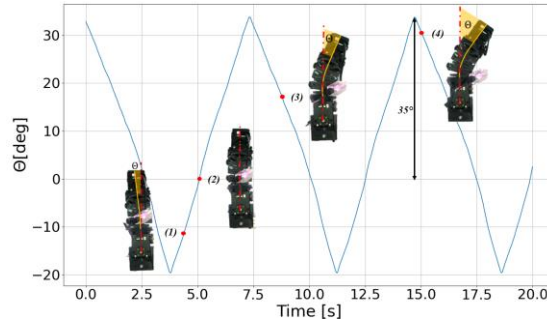


Fig. 14. Absolute angle achieved by the module.

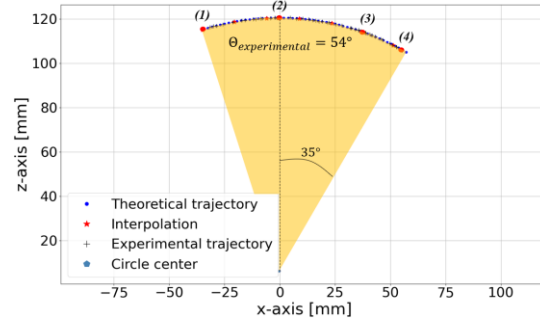


Fig. 15. Experimental and theoretical trajectories (arc planar motion in  $\mathbf{XZ}$ ). Height along Z-Axis is about 120 mm (height of marker  $m_1$  fixed on servomotor 2).

The second theoretical trajectory was a circle that mimics snakes' swimming motion in a 3D space. Pulleys angles  $\gamma_1$  and  $\gamma_3$  actuated by servomotor 2 are antagonistic as they are conversely wound to the same pulley. Idem, pulley angles  $\gamma_2$  and  $\gamma_4$  are actuated by servomotor 1. Both servomotor 1 and servomotor 2 are actuated.

Figure 16 shows both, experimental and theoretical trajectories. Theoretical (expected) circular trajectory with a radius of 112 mm in the horizontal plane at  $z = 115\text{mm}$ , and experimental (observed) trajectory were compared (Fig. 16). Experimental trajectory was circular, the movement was complete without discontinuity or irregularity. Moreover, experimental, and theoretical trajectories overlapped despite a slight positional error. Figure 16 shows the different configurations of the module performing a circle. The module shows the capability to move in a volume that corresponds to the inspired motion of swimming snake.

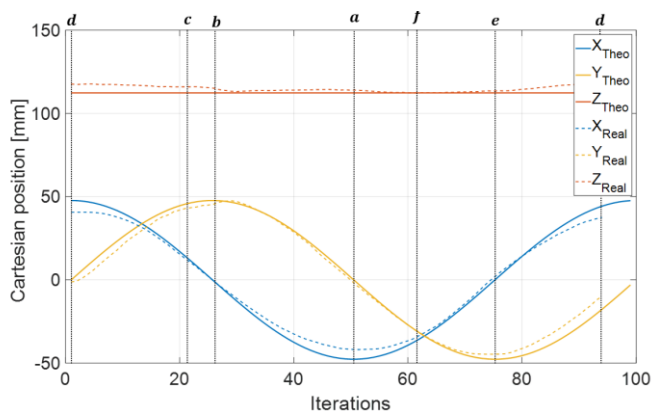


Fig. 16. Deviation of experimental trajectory ( $x_{real}$ ,  $y_{real}$ ,  $z_{real}$ ) according to the theoretical trajectory ( $x_t$ ,  $y_t$ ,  $z_t$ ) over time.

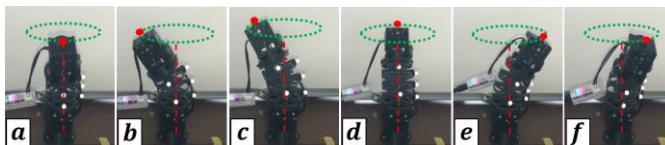


Fig. 17. Different bending cases to achieve circle trajectory, theoretical trajectory in green and end-effector point in red.

## B. Discussions

In this study, a two DoF bio-inspired HCDR module was actuated with antagonistic cables driven by two servomotors and placed in horizontal position. The experiments highlighted the module's capability to move in a plane as well as in a volume while respecting the amplitude of the radius of the circle's arcs measured on real swimming snakes. In a plane, HCDR module's movements encompassed the range of angles observed in snakes segmented into 11 sections during measurements (Table 2). Zero-point cable-driven robot was adjusted with the pulley and an offset defined in the control program enabled precise alignment. Cables tension was ensured by tensioning system and elasticity of the flexible module (BFM). During experimental tests mechanical stop was achieved with the contact between flexible vertebrae. This interaction might create friction for wide angles and may disturb motion fluidity. This issue will be considered in future work. We expect that, if positioned horizontally, the HCDR module will behave as well as it did vertically (i.e., will produce trajectories similar to, or very close to, theoretical trajectories). In the horizontal position, bending issues may appear; but they might be compensated through controlling the initial cable tension. We also expect that when the module will be immersed, gravity will be compensated by interaction force between the fluid and the module, especially when assembling a multi-modular robot.

## V. FUTURE WORK

The approach used in this study was fundamentally based on precise analysis of real swimming snakes. Although, the results presented in this work are preliminary, the outcome highlights that key biological movements were accurately mimicked. However, swimming snake undulatory locomotion characteristics cannot be merely assimilated to only 3 snakes and 2 species. Thus, further measurements on various species (aquatic and terrestrial snakes) and multiple individuals within each species (>10 sequences/snake) are needed to produce more meaningful and comprehensive movements usable for biologists and roboticists. A larger data set will provide robust basis to improve the biomimicry design of an optimized module. Notably, it will permit an iterative process (positive feed-back) of design-experimentation-comparisons between the bio-inspired module and the analysis of kinematics gathered in living snakes during swimming.

Regarding the comparisons of theoretical, numerical, and experimental results, the behavior of the Bio-inspired Flexible Module (BFM) was satisfactory, but it needs to be improved for a better correlation of the deformations of animals versus robot body. This can be done by modifying the material, the shape of the module or the wall thicknesses.

The simple conception of the bio-inspired HCDR module opens opportunities for various improvements. Waterproofing the module is required to perform tests underwater or at water surface. Thus, a bio-inspired artificial skin will be developed and integrated to the HCDR module. Motion control will be adapted to accurately reproduce swimming snake locomotion especially for significant angles ( $\theta > 50^\circ$ ).

Finally, the assembly of HCDR modules in series will constitute the snakebot: a waterproof swimming snake robot composed of multiple HCDR modules homogeneously distributed along the robot snake's body. Finally, we will investigate the motion control of multiple joints using various methods such as kinematic and dynamic models.

## VI. CONCLUSION

This paper presents a biomimetic (biospired) approach and the design as well as the experimental validation of a new bio-inspired flexible hybrid cable driven robot (HCDR). The first step was to examine the anatomy and swimming locomotion of

snakes (i.e., snake analysis paragraph). Then skeleton' DoFs and curvature of swimming snakes were characterized and implemented in the design of a bio-inspired HCDR module.

The key contributions of this paper can be summarized as:

- 1) A novel bio-inspired HCDR module design based on the association of rigid and flexible modules enables to balance the distribution of motors (mass distribution). This design allows the association of multiple HCDR modules to form an autonomous swimming snake robot. Cable driven design is inspired from linkage between muscles, tendons, and vertebrae of living snakes. To the best of our knowledge, such a hybrid design that associates a servomotor and a flexible module with compliant joints as standard, is novel.
- 2) A bio-inspired flexible module has been developed and tested. Arc curvature observed in biological snakes were accurately reproduced with constant curvature flexible module based on Rigid Body Replacement method. Flexion-extension and lateral bending motions were reproduced through compliant joints.
- 3) Close collaboration between biology and robotics was required to reproduce snake swimming locomotion and snake's skeleton curvature obtained in real snakes.

As a result, the bio-inspired HCDR module offers the advantages of being modular, well mimicking snake by reproducing fluid curvature on a section frictionless thanks to flexible joint that can move in three dimensions. The use of a one-piece flexible module greatly facilitates prototype assembly. Rigid and flexible cable driven module combinations offer ample possibilities to design different sized modules to encompass the variability of snake body size (from minute blind-snakes species to large pythons) and to reproduce the complete snake undulations. Importantly, the adopted design strategy reduces the number of actuators and consequently reduces the weight of the whole system.

#### ACKNOWLEDGMENT

This research was funded by the French government by means of National Research Agency (ANR). This research is part of ANR DRAGON-2 project (ANR-20-CE02-0010).

#### REFERENCES

- [1] J. M. Benyus, *Biomimicry: innovation inspired by nature* /. Perennial, 2002.
- [2] T.-Y. Ning *et al.*, 'Biomimetic mineralization of dentin induced by agarose gel loaded with calcium phosphate', *J Biomed Mater Res B Appl Biomater*, vol. 100, no. 1, pp. 138–144, Jan. 2012
- [3] R. Salazar, V. Fuentes, and A. Abdelkefi, 'Classification of biological and bioinspired aquatic systems: A review', *Ocean Engineering*, vol. 148, pp. 75–114, Jan. 2018
- [4] S. Hirose and M. Mori, 'Biologically Inspired Snake-like Robots', in *2004 IEEE Int. Conf. on Rob. and Biomimetics*, Shenyang, China, 2004, pp. 1–7
- [5] A. J. Ijspeert, 'Amphibious and Sprawling Locomotion: From Biology to Robotics and Back', *Annual Review of Control, Robotics, and Autonomous Systems*, vol. 3, no. 1, pp. 173–193, 2020
- [6] Y. Munk, 'Kinematics of swimming garter snakes (*Thamnophis sirtalis*)', *Comp Biochem Physiol A Mol Integr Physiol*, vol. 150, no. 2, pp. 131–135, Jun. 2008
- [7] G. B. Gillis, 'Undulatory Locomotion in Elongate Aquatic Vertebrates: Anguilliform Swimming since Sir James Gray', *Am Zool*, vol. 36, no. 6, pp. 656–665, Dec. 1996
- [8] F. Brischoux, A. Kato, Y. Ropert-Coudert, and R. Shine, 'Swimming speed variation in amphibious seasnakes (Laticaudinae): A search for underlying mechanisms', *J. of Exp. Marine Biology and Ecology*, vol. 394, no. 1, pp. 116–122, Oct. 2010
- [9] K. Karakasiliotis *et al.*, 'From cineradiography to biorobots: an approach for designing robots to emulate and study animal locomotion', *Journal of The Royal Society Interface*, vol. 13, no. 119, p. 20151089, Jun. 2016
- [10] F.-C. Li and K. Hishida, 'Chapter 3 Particle Image Velocimetry Techniques and its Applications in Multiphase Systems', in *Ad. in Chemical Engineering*, vol. 37, J. Li, Ed. Academic Press, 2009, pp. 87–147
- [11] B. C. Jayne, 'Muscular mechanisms of snake locomotion: an electromyographic study of the sidewinding and concertina modes of *Crotalus cerastes*, *Nerodia fasciata* and *Elaphe obsoleta*', *J Exp Biol*, vol. 140, pp. 1–33, Nov. 1988.
- [12] H. A. Abdel-Aal, M. El Mansori, and S. Mezghani, 'Multi-Scale Investigation of Surface Topography of Ball Python (*Python regius*) Shed Skin in Comparison to Human Skin', *Tribol Lett*, vol. 37, no. 3, pp. 517–527, Mar. 2010
- [13] F. Boyer, D. Chablat, P. Lemoine, and P. Wenger, 'The Eel-Like Robot', in *Volume 7: 33rd Mechanisms and Robotics Conference, Parts A and B*, San Diego, California, USA, Jan. 2009, pp. 655–662
- [14] A. Crespi and A. J. Ijspeert, 'AmphiBot II: An Amphibious Snake Robot that Crawls and Swims using a Central Pattern Generator', *Proceedings of the 9th Int. Conf. on Climbing and Walking Robots*, Jan. 2006.
- [15] P. Liljeback, O. Stavdahl, K. Y. Pettersen, and J. T. Gravdahl, 'Mamba - A waterproof snake robot with tactile sensing', in *2014 IEEE/RSJ Int. Conf. on Int. Rob. and Systems*, Chicago, IL, USA, Sep. 2014, pp. 294–301
- [16] M. Porez, F. Boyer, and A. J. Ijspeert, 'Improved Lighthill fish swimming model for bio-inspired robots: Modeling, computational aspects and experimental comparisons', *The Int. J. of Robotics Research*, vol. 33, no. 10, pp. 1322–1341, Sep. 2014
- [17] N. Kamamichi, M. Yamakita, K. Asaka, and Z.-W. Luo, 'A snake-like swimming robot using IPMC actuator/sensor', in *Proceedings 2006 IEEE Int. Conf. on Rob. and Automation, ICRA.*, May 2006, pp. 1812–1817

- [18] H. Jiang, X. Liu, X. Chen, Z. Wang, Y. Jin, and X. Chen, 'Design and simulation analysis of a soft manipulator based on honeycomb pneumatic networks', 2016, IEEE, ROBIO, pp.350-356
- [19] P. Qi, C. Qiu, H. Liu, J. S. Dai, L. D. Seneviratne, and K. Althoefer, 'A Novel Continuum Manipulator Design Using Serially Connected Double-Layer Planar Springs', *IEEE/ASME Transactions on Mechatronics*, vol. 21, no. 3, pp. 1281–1292, Jun. 2016
- [20] Z. Li and R. Du, 'Design and Analysis of a Bio-Inspired Wire-Driven Multi-Section Flexible Robot', *Int. J. of Ad. Robotic Systems*, vol. 10, no. 4, p. 209, Apr. 2013
- [21] E. Kelasidi, *Modeling, Control and Energy Efficiency of Underwater Snake Robots*. NTNU, 2015
- [22] J. A. Gallego and J. Herder, 'Synthesis Methods in Compliant Mechanisms: An Overview', Jul. 2010, pp. 193–214
- [23] F. Galbusera and T. Bassani, 'The Spine: A Strong, Stable, and Flexible Structure with Biomimetics Potential', *Biomimetics (Basel)*, vol. 4, no. 3, p. 60, Aug. 2019
- [24] A. Pattishall and D. Cundall, 'Dynamic changes in body form during swimming in the water snake *Nerodia sipedon*', *Zoology*, vol. 111, no. 1, pp. 48–61, Jan. 2008
- [25] M. Sfakiotakis, D. M. Lane, and J. B. C. Davies, 'Review of fish swimming modes for aquatic locomotion', *IEEE J. of Oceanic Engineering*, vol. 24, no. 2, pp. 237–252
- [26] B. P. Trease, Y.-M. Moon, and S. Kota, 'Design of Large-Displacement Compliant Joints', *J. of Mechanical Design*, vol. 127, no. 4, pp. 788–798, Nov. 2004